PLASMA RESEARCH

CASE INSTITUTE OF TECHNOLOGY

UNIVERSITY CIRCLE • CLEVELAND 6, OHIO

NSG-198
NSR-(T)-42

THE HOLLOW CATHODE DISCHARGE APPLIED TO LASER DESIGN

by

Thomas F. Trost*
W. B. Johnson

Technical Report A-46

*National Aeronautics and Space Administration Graduate Traineeship.

ACKNOWLEDGMENTS

The authors wish to express their appreciation of the expert work of the glass blowers, Mr. Edward V. Parillo and Mr. Imre Szilagyi, and the help given by Jeanette Yount and Theresa Trost in typing the report.

ABSTRACT

The possibility of achieving laser action in the sputtered metallic vapor of a hollow cathode glow discharge is investigated. Intensity measurements are carried out on the spectral lines emitted by the vapor in the cathode region of copper and iron hollow cathode tubes. The measurements are analyzed using a graphical technique designed for identifying inverted excited state populations. The method is limited by a lack of known gf-values for ionic states. In the literature, various possibilities for resonance collisions between sputtered metal ions and carrier gas atoms are discovered. A suitable copper-helium collision is found for achieving a population inversion among the excited states of copper ions. A copper cathode laser is constructed, but laser action is thus far not observed.

TABLE OF CONTENTS

LIST OF FIGURES AND TABLES

CHAPTER I

INTRODUCTION

1.1 Purpose of the Research

As the quest for new laser materials continues, leaving in its wake a multitude of wavelengths at which oscillation has been achieved, the designer of practical laser systems for communications, medicine, industry, or basic research finds an ever-increasing wealth of lasers to choose from. Laser action has now been obtained over a wavelength range extending from the ultraviolet up to a sizeable fraction of a millimeter. Research has already expanded from the realm of atomic physics into the laboratory of the chemist, who now speaks optimistically of a chemical laser. Clearly, the task of endeavoring to discover new laser transitions is an exciting and often rewarding one.

The purpose of the work described in this report is to search for excited state population inversions in metals in electric discharges. Any sufficiently pronounced inversion, it is thought, may lead to realization of a new laser transition. The ultimate goal is the construction of a laser operating on such a transition.

The preliminary studies aimed at finding non-thermal populations were carried out by spectroscopic means in the laboratory and

by examining data available in the literature. The majority of the laboratory work consisted of measuring and comparing spectral line intensities in the spectrum of atomic copper and in atomic iron. The measurements yielded information about excitation mechanisms within the discharges and demonstrated the feasibility of a graphical technique for spotting non-thermal population densities. The technique is at present limited, though, because of insufficient knowledge of the atomic constants (gA-and gf-values) which are involved. The method is not easily applied, for example, to the spectrum of CuII, a spectrum which is of interest when seeking evidence of non-thermal populations.

It was found, therefore, that the possibilities for inverted populations were best examined through the literature. Here some methods were found for selectively populating given levels in singly ionized aluminum and copper. A laser with an active medium of copper was subsequently built, with a view toward achieving oscillations on a CuII transition in the blue-green at 4909 Å ($4f\,^3H_6 \rightarrow 4d\,^3G_5$). One of the reasons for choosing copper as opposed to aluminum involves relative sputtering rates and will be made clear in section 1.4. At the writing of this report, laser action has not yet been obtained on the copper transition. Details of the copper laser design are to be found in Chapter 5.

1.2 Outline of the Spectroscopic Technique

The general laboratory technique employed by us in looking for inverted populations has been used to some extent in the past by spectroscopists for determining atomic transition probabilities and by astronomers in measuring the temperatures of stars. Basically the method is one of comparing the intensities of the lines in the spectrum emitted by an excited gas or vapor. For determining transition probabilities, the emission from the vaporized metal between the electrodes of a laboratory electric arc is often studied; while for astronomical temperature measurements, the observed gas would be one of the constituents of the atmosphere of a star.

In the present report our attention is focused on the spectrum of the light emitted from within a hollow cathode, glow discharge tube. Three noble gases, helium, neon, and argon, are used at pressures in the neighborhood of 4 mmHg. Direct current flows through the tube between metal electrodes, giving rise to a visible glow, characteristic of the particular gas employed. However, it has been known for perhaps fifty years[1] that the glow in a tube of the hollow cathode type may contain not only the emission lines of the gas but also spectral lines of the cathode material. These are the lines which are studied; they appear not throughout the entire discharge but only in the region of the cathode.

It is thought that the cathode spectrum is excited in two

steps according to the following scheme: (1) Metal atoms are ejected from the cathode surface by the shower of positive noble gas ions impinging on the cathode. This phenomenon, known as sputtering, is in many cases one of momentum transfer and is expected to be most pronounced when the ion mass equals that of the surface atom.[2] The sputtering rate is also enhanced by the geometry of the hollow cathode.[3] (2) Once driven into the gas phase, the metal atoms collide inelastically with gas particles (neutral atoms, ions, and electrons) and are excited to spectral emission. The collisions that one expects to be most effective in this process are those between metal atoms and electrons, since it is for these that the relative velocity between colliding particles, and thus the collision cross section, are the largest.

By imaging the light from the vicinity of the cathode into a suitable spectrometer, one can measure the intensity of each line emitted by the cathode material. An analysis of the line intensities is then carried out in a manner which involves various atomic constants and is described in detail in Chapter 2. In essence, the analysis leads to a graph of the logarithm of line intensity, normalized in a certain sense, versus the upper state excitation potential. That is, each spectral line is represented graphically by a point having as an ordinate the logarithm of the normalized line intensity and an abscissa equal to the excitation potential of the upper atomic state involved in the transition that

produces the line. It is from this graph that conclusions may be drawn regarding the presence of population inversions among the various excited states. One such graph is shown on page 32.

Theory shows that if the metal vapor is excited through collisions with electrons and the electrons are in thermal equilibrium, then the points on the graph will fall on a straight line with negative slope. This result corresponds to a Maxwell-Boltzmann distribution of electron energies and is derived in Chapter 2. It has been confirmed experimentally in our laboratory. However, the presence of certain types of collisions between metal and gas atoms, in addition to the metal atom--electron collisions, can alter the distribution of excited states in the metal vapor by heavily populating a few specific levels. These are the so-called resonance collisions, or collisions of the second kind, which involve an interchange of excitation energy between the two colliding particles--in the present case, a transfer of energy from the noble gas atom to the metal atom. If such processes are occurring within the discharge, the graph points will, in general, no longer form a straight line. A single resonance collision process, for example, could probably be recognized as a single graph point significantly displaced from the line formed by the other points. Such a situation is just what is required for laser action and is precisely what we looked for in the laboratory; it corresponds to a possible inversion of the populations of two excited states in the metal

vapor. The resonance collision processes that are to be considered are

$$A^* + M \rightarrow A + (M^+)^* + e$$

or

$$A^+ + M \rightarrow A + (M^+)^*,$$

where A^* and A^+ signify excited and ionized gas atoms respectively and M and $(M^+)^*$ indicate metal atoms and excited metal ions.

1.3 Construction of a Laser

Once selective populating of a particular level is found from the intensity graph to be appreciable under reasonable operating conditions, there is the possibility of constructing a laser oscillating at the wavelength represented by the anomalous point on the graph. To obtain laser action, it is necessary to achieve a sufficient population inversion, that is, to have more atoms in the higher of the two levels connected by the radiative transition. The upper level must be efficiently filled and the lower efficiently emptied. Consider a metallic ion such as CuII. The overpopulation of the upper level might be due to collisions with rare gas atoms; while rapid depopulation of the lower level would result, one might

expect, by radiative decay to a lower state followed by recombination of the copper ions with electrons to form neutral Cu atoms.

It is possible, then, to imagine a metal laser consisting of a long metallic tube with a glass bulb sealed to each end. Each bulb would contain an anode and would accommodate a Brewster-angle window for satisfactory transmission of the laser beam. Two parallel discharges would be run with the metal tube connected as the common cathode for both. With the tube positioned in a Fabry-Perot cavity, laser oscillation would be stimulated in the sputtered metal vapor through resonance collisions with noble gas atoms.

1.4 Suitable Metals

The sputtering process discussed above will in general proceed at different rates for different metals. Some metal surfaces are easily vaporized through sputtering while others remain rather impervious to the ion bombardment. Having in mind the eventual construction of a laser operating on a metal vapor transition, one looks for metals that sputter readily. Among these are gold, silver, copper, and bismuth.[4] The sputtering rates of aluminum and magnesium, by way of contrast, are quite low. Copper has additional advantages in that it can if necessary be sealed to glass and is inexpensive. Also in the favor of copper is the fact that an excellent analysis of the hollow cathode spectrum of CuII in He and in Ne has been carried out by Shenstone,[5] representing a valuable

source of data on copper population inversions.

Because of its suitability, copper is the focal point of interest in this report. Only in two cases are other metals discussed: (1) The spectrum of atomic iron was looked at briefly in the laboratory and a spectral line intensity graph was plotted. It appears with similar graphs for copper in Chapter 4. (2) A collision process was found whereby a given level in AlII might be selectively excited by collisions with neon ions. The process is discussed at the end of Chapter 3.

1.5 Contents of the Report

The essential content of each chapter is noted here to serve as a guide to the reader. Chapter 2 is concerned with the mathematics behind the straight-line graphs presented later in the report. A brief derivation is given, based on an assumed Maxwellian distribution of electron energies, which leads directly to the desired linear relationship between the logarithm of the spectral line intensity and the upper state energy. In Chapter 3 is a discussion of collision processes and in particular of resonance collisions that can be identified by studying available spectroscopic data. Chapter 4 deals with the discharge tubes used in taking spectroscopic measurements, their operation and construction. The straight-line intensity plots are included here along with other

data of interest, such as gas clean-up rate and spectral line intensities as a function of current and pressure. Chapter 5 describes our copper laser design and mentions operating characteristics of the laser tube and some of the problems encountered. Chapter 6 summarizes results and discusses future work.

CHAPTER II

THEORETICAL FORMULATION

2.1 The Maxwell-Boltzmann Distribution

In elementary texts on thermodynamics the arguments presented are often based on the macroscopic description of systems in thermodynamic equilibrium. No special assumptions are made concerning the internal structure of the materials involved. Gross characteristics are studied by dealing with a small number of macroscopic coordinates, such as temperature, pressure, and volume, in the case of an ideal gas, and relationships between these quantities are derived.

On the other hand, it is possible to approach the subject of thermodynamics from a statistical point of view wherein the system under consideration is imagined to consist of a very large number of tiny microsystems, each of which may exist in any one of a number of energy states. This microscopic view goes beyond the specification of measurable quantities and delves into the basic structure of matter. When the system to be studied is a gas, the microsystems are the molecules of the gas. One might ask how many molecules there are on the average in each available energy state, given that the system has a specified total energy and total number of molecules.

In the case of a dilute gas in thermodynamic equilibrium, the answer is that the overwhelmingly most probable distribution of molecules among their own individual states is the Maxwell-Boltzmann distribution:

$$n_i \propto e^{-\frac{E_i}{kT}}, \qquad (2.1)$$

where n_i is the number of molecules per unit volume with energy E_i, k is Boltzmann's constant, and T is the absolute temperature. Consider now the electron gas within a DC glow discharge tube. The electrons are drifting toward the anode under the influence of a steady electric field. In the neighborhood of the cathode they collide with metal atoms sputtered from the cathode surface and with gas atoms and ions. Can it be said that the electrons are in local thermodynamic equilibrium near the cathode? In general, one would think of answering this question in the affirmative only if the electric field were quite weak and the gas pressure sufficiently high. The electrons would then gain negligible energy from the field, relative to their thermal energy, in the intervals between collisions. A near-equilibrium situation could exist, and a Maxwell-Boltzmann distribution of electron energies would be expected.

2.2 Intensity Ratios of Spectral Lines

At this point we assume, for the purpose of a theoretical discussion, a local Maxwell-Boltzmann distribution for electrons near the cathode in a discharge tube of the hollow cathode type used for this experiment. An analysis will be set down which predicts the sort of results one might obtain when making spectral measurements on the tubes. It predicts for the metal spectra the straight-line graphs mentioned in Chapter 1.

It must be noted here that we did not, at the outset of our research, know how closely the data would approximate the result expected for a Maxwellian distribution. Calculations which would predict whether or not equilibrium prevails in our case are not reliable because of the difficulty in accurately estimating the electric field strength and the collision rate.

As electrons collide with free metal atoms within the discharge, the excited states of the atoms are being populated and depopulated. With a sufficiently large electron density, both excitation and de-excitation of atomic levels is due primarily to atom-electron collisions, although some excitation energy is given up in the form of radiation in the visible and ultraviolet. Just as the electrons have a Maxwellian distribution of energies characterized by a temperature T, so too are the excited states of the atoms populated according to this distribution. Not a great deal of kinetic energy is imparted to the metal atoms by electrons

because the mass of a metal atom is so much greater than that of an electron.

In the metal vapor cloud the number of metal atoms per unit volume in the i-th excited state is proportional to $e^{-\frac{E_i}{kT}}$, from Equation 2.1, as long as the a priori probability of being in any one of the states is the same. It is well known, however, that with each state can be associated a definite statistical weight, g_i, which gives essentially the a priori probability for the state. Thus, for the state i, the number density of atoms is

$$n_i \propto g_i e^{-\frac{E_i}{kT}} ;$$

or, introducing the proportionality constant K,

$$n_i = K g_i e^{-\frac{E_i}{kT}} . \qquad (2.2)$$

The intensity, I, of a spectral line emitted by the metal vapor in watts/cm^3 is given by the product of the energy contained in each photon emitted, $h\nu$, and the rate of photon emission per unit volume. The photon emission rate is equal to the rate at which n_i decreases due to radiative decay at frequency ν. We call

this rate $(\frac{dn_i}{dt})_\nu$, whence

$$I = h\nu(\frac{dn_i}{dt})_\nu \ . \qquad (2.3)$$

The derivative with the subscript ν represents only the radiative depopulating of n_i into a given lower state, not the total rate of change of n_i. The derivative of n_i without the subscript, $\frac{dn_i}{dt}$, is the total rate of change of the population of state i with time.

Neglecting stimulated emission, the decay rate of Equation 2.3 is just proportional to n_i through a constant, A_{ij}, customarily called the Einstein A coefficient or Einstein probability. Thus

$$(\frac{dn_i}{dt})_\nu = A_{ij}\ n_i \ . \qquad (2.4)$$

The Einstein coefficient is simply the spontaneous transition probability for the transition $i \rightarrow j$. Combining Equations 2.2, 2.3 and 2.4 yields the following relation for the spectral line intensity I:

$$I = h\nu A_{ij} K g_i e^{-\frac{E_i}{kT}} \ . \qquad (2.5)$$

After setting $\nu = \frac{c}{\lambda}$ and rearranging coefficients slightly, the above equation can be written as follows:

$$\frac{I\,\lambda}{g_i A_{ij}} = hcK\, e^{-\frac{E_i}{kT}}$$

Taking the natural logarithm of both sides and then converting to logarithms to the base 10 gives

$$\log\left(\frac{I\,\lambda}{g_i A_{ij}}\right) = \log(hcK) - \frac{1}{2.30}\,\frac{1}{kT}\,E_i \ , \qquad (2.6)$$

where the factor 2.30 is due to the conversion to base 10. The quantity $\frac{I\,\lambda}{g_i A_{ij}}$ can, in a sense, be thought of as a corrected, or weighted, intensity. It is the intensity of a line, with proper weighting for comparison with other line intensities. We adopt the following notation for the sake of brevity:

$$\frac{I\,\lambda}{g_i A_{ij}} \equiv I_w$$

The subscript w will hereafter signify that the intensity, I, has been weighted by the factor $\frac{\lambda}{g_i A_{ij}}$.

The term log(hcK) in Equation 2.6 will be a constant for any given spectrum so that we may write Equation 2.6 as

$$\log(I_w) = \text{const.} - \frac{1}{2.30\ kT} E_i \ . \qquad (2.7)$$

This result shows explicitly that a graphical plot of $\log(I_w)$ versus E_i for a number of emission lines in a given spectrum will theoretically give a straight line. The slope of the line will be $-\frac{1}{2.30\ kT}$. Equation 2.7 then, is the principal result of this chapter of the report.

2.3 Formulation with the gf-value

Equation 2.5 of the previous section can be cast into an alternate form wherein the Einstein coefficient does not appear. This is done by introducing a quantity known as the oscillator strength, f_{ji}, which is related to the absorption of radiation of frequency ν through the transition $j \rightarrow i$ rather than emission through the decay $i \rightarrow j$. Recall that we have labeled the upper level i and the lower j for the radiative transition at frequency ν. The magnitude of the oscillator strength tells one how efficiently the atom absorbs energy of this frequency. It can be shown[6] that f_{ji} is related to A_{ij} according to

$$f_{ji} = \frac{mc^3}{8\pi^2 q^2 \nu^2} \frac{g_i}{g_j} A_{ij} \ ,$$

where m is the mass of an electron and q the electron charge. The statistical weight g_j applies to the lower state, j, just as g_i corresponds to the state i. In terms of the oscillator strength, Equation 2.5 can be written

$$I = \frac{8\pi^2 q^2 hK}{m\lambda^3} g_j f_{ji} \, e^{-\frac{E_i}{kT}} \ .$$

This equation leads directly to Equation 2.7, with I_w now defined as $\frac{I\lambda^3}{g_j f_{ji}}$. The product $g_j f_{ji}$ is a well known quantity referred to in the literature simply as the gf-value.

One might ask why we introduce the base 10 logarithms, which necessitate the constant 2.30 in Equation 2.7, instead of using logs to the base e and avoiding this additional factor. This is done only for the following reason: Tabulated values of the quantity $\log_{10}$gf are published by the National Bureau of Standards;[7] these are used in plotting all our data. It is thus more convenient to plot directly in base 10 logarithms using the NBS data than to convert each $\log_{10}$gf-value to the base e and plot in the base e.

CHAPTER III

INVERTED POPULATIONS EVIDENCED IN THE LITERATURE

3.1 Criterion for Resonance Collisions

A wide variety of collision processes may occur simultaneously within a gas discharge of the kind described in Chapter I. One way to discover which processes are most important in a given situation is to examine the light emitted from the luminous gas. Through the use of spectroscopy one can delve into the physics of the discharge, passing from the realm of the simple beauty of the colors to that of the dominant atomic phenomena.

In order to interpret accurately the spectroscopic data taken in the laboratory, a familiarity with possible collision processes is necessary. For the present research our interest mainly lies in collisions between metals and rare gases. In particular, the following collisions are important because they provide a means of selectively populating a given state in the metal ion:

1. $Cu + Ne^{+} \rightarrow (Cu^{+})^{*} + Ne + \text{kinetic energy}$
2. $Cu + Ne^{*} \rightarrow (Cu^{+})^{*} + Ne + e^{-} + \text{kinetic energy}.$

Here the asterisk represents a particular excited state of the atom

or ion. While copper and neon can indeed collide as shown, they are used by way of example only; a great variety of metals might in practice be found to undergo such collisions, with various gases.

The first collision is the charge transfer process wherein an electron leaves the copper atom to join the neon atom. The copper ion thus created is in a particular excited state and may subsequently decay by photon emission to a lower state. The second collision process involves an interchange of excition energy between a metastable neon atom and a copper atom. Again, the result of these collisions is to leave the copper ions with a preferentially populated level.

The two processes listed above, which are among the class of collisions known as resonance collisions (collisions of the second kind), occur only when the excitation energy of the recoiling metal ion very nearly equals the internal energy of the incident noble gas atom. The energy level coincidence must be, in fact, of the order of kT or less, where T is the absolute gas temperature. It is just this type of collision that makes possible the He-Ne laser.

Figure 1 illustrates the required matching of energy levels for each of the two collisions. For the specific example given, i.e., copper-neon collisions, the energy coincidence for process 1 is 0.155 ev; while for process 2, ΔE is only 0.0028 ev. In the figure most of the levels of neon and copper have not been drawn, for the sake of simplicity. The ionization potential of

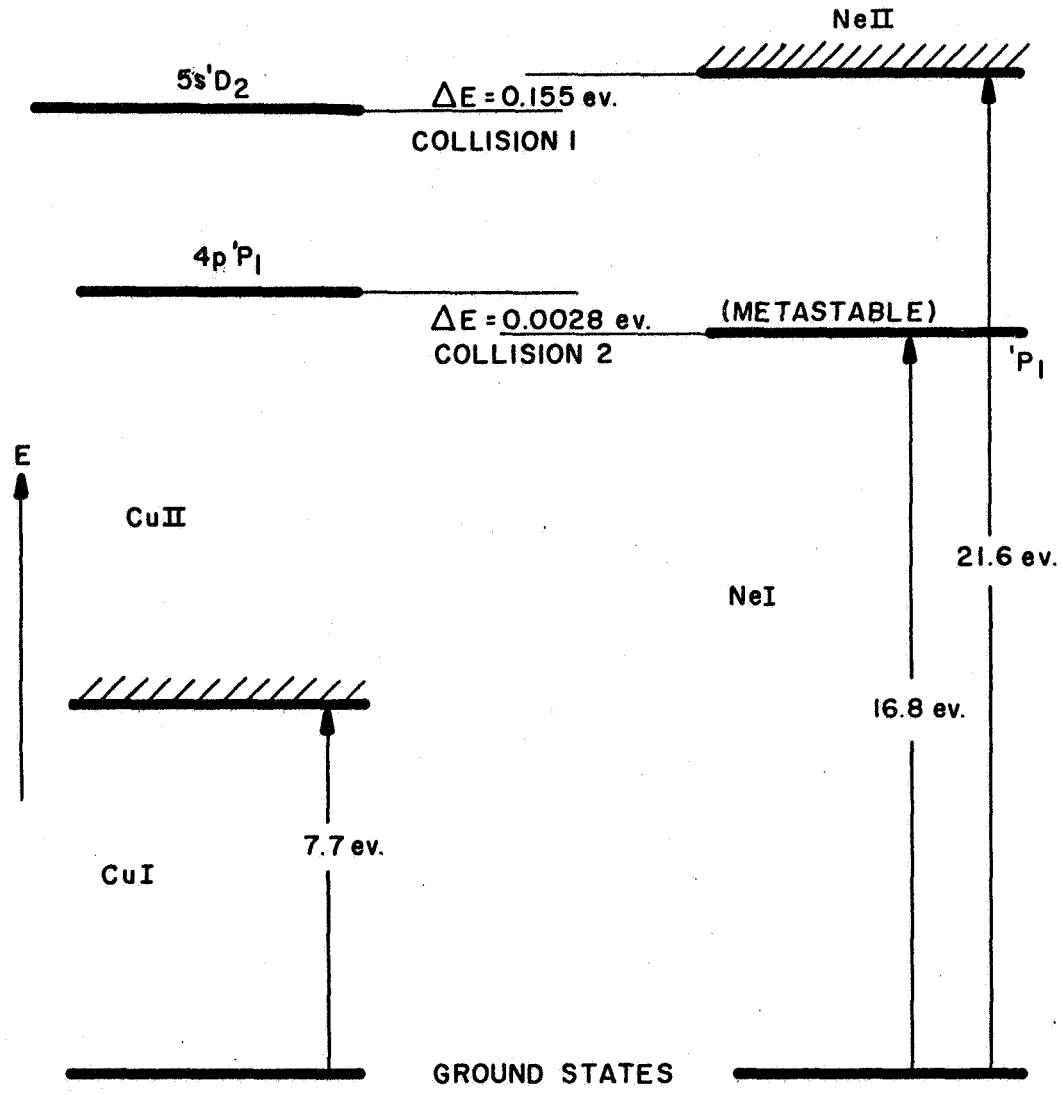

Figure 1. Copper-Neon Energy Resonances

Cu II lies at 20.29 ev above the Cu II ground state.

3.2 Specific Collisions

3.2 a Copper

The energy levels of the excited states of Cu II are given in NBS Circular 467, Volume II. In order to determine whether or not a collision of type 1 can occur in Cu II in the presence of a noble gas, the ionization potentials of the gases are compared to the energies of the copper states. Considering a copper atom temperature of 400°K, the energy (kT) is roughly 0.034 ev; so the levels must be coincident to within a few hundreths of an ev or to within about 500 cm^{-1}. The 400° temperature is a typical atom temperature for glow discharges. The ionization potentials of He, Ne, A, Kr, and Xe are given in Table 1.

TABLE 1

NOBLE GAS IONIZATION POTENTIALS

He	24.58 ev
Ne	21.559 ev
A	15.755 ev
Kr	13.996 ev
Xe	12.127 ev

Shenstone[8] has catalogued the lines that appear in the spectrum of Cu II when a hollow copper cathode discharge is run in helium and in neon. Relative intensity and upper and lower term designations are given along with the wavelength of each line. This data was employed by us in the following manner: Each time an energy coincidence of type 1 was found by comparing copper levels and rare gas ionization potentials, an optical transition downward from the Cu II level was sought. This would become the lasing transition if a laser were built to utilize the particular type 1 collision. A summary of our research on charge transfer (type 1) collisions in copper is given in Table 2. Note that a number of lines may be excited by collisions in any one of the three gases, helium, neon, and argon. Only in helium, however, is the energy coincidence small enough to permit effective collisions at 400°K.

Recall that the lower laser level must always be depopulated quickly to assure that the inverted character of the upper and lower state population densities is preserved. Since radiative decay is a fast depopulating mechanism, we require that there be allowed optical transitions downward from the lower level. It can be verified from Shenstone's data that the $4d^3G_5$ and $4d^3G_4$ states, which become filled as a result of the He-Cu resonance, do indeed decay optically. The two states are singled out and specifically checked for radiative decay because the lines at 4909 and 4931 which fill these states are among the strongest lines in Shenstone's

entire Cu II spectrum and as such are of primary interest as possible laser wavelengths. The various other lower levels, $4d^3D_3$, $4d^3D_2$, etc., which may be populated through the helium collision have not been checked for downward optical transitions since the transitions to these states are very weak, according to Shenstone, compared to the lines at 4909 and 4931.

TABLE 2

CHARGE TRANSFER COLLISIONS IN COPPER (Cu II)

Noble Gas	Energy Level Difference ΔE (cm^{-1})	Transitions Excited: Classification	Transitions Excited: Wavelength (Å)
He^+	57	$4f^3H_6 \rightarrow 4d^3G_5$	4909.726
	54	$4f^3H_5 \rightarrow 4d^3G_4$	4931.653
	0	$4f^3D_3 \rightarrow 4d^3D_2$	5100.08
	0	$4f^3D_3 \rightarrow 4d^3D_3$	5021.285
	0	$4f^3D_3 \rightarrow 4d^3F_3$	5083.991
	0	$4f^3D_3 \rightarrow 4d^3P_2$	4912.362
	0	$4f^3D_3 \rightarrow 4d^3F_4$	5095.746
	30	$4f^1P_1 \rightarrow 4d^1S_0$	7382.18
	30	$4f^1P_1 \rightarrow 4d^3P_0$	5158.090
	30	$4f^1P_1 \rightarrow 4d^3D_2$	5108.331
	30	$4f^1P_1 \rightarrow 4d^3P_1$	4926.390
	30	$4f^1P_1 \rightarrow 4d^3P_2$	4920.031

Table 2 continued

Noble Gas	Energy Level Difference ΔE (cm^{-1})	Transitions Excited: Classification	Transitions Excited: Wavelength (Å)
	26	$4f^3D_2 \rightarrow 4d^3D_2$	5093.792
	26	$4f^3D_2 \rightarrow 4d^3F_3$	5077.805
	26	$4f^3D_2 \rightarrow 4d^3D_3$	5015.207
Ne^+	1248	$5s^1D_2 \rightarrow 4p^1P_1$	2718.775
	1248	$5s^1D_2 \rightarrow 4p^1D_2$	2700.963
	1248	$5s^1D_2 \rightarrow 4p^1F_3$	2600.266
	1248	$5s^1D_2 \rightarrow 4p^3D_2$	2571.746
	1530	$5s^3D_1 \rightarrow 4p^1P_1$	2739.768
	1530	$5s^3D_1 \rightarrow 4p^1D_2$	2721.675
A^+	1626	$4p^3P_2 \rightarrow 4s^1D_2$	2489.652
	1626	$4p^3P_2 \rightarrow 4s^3D_1$	2356.638
	1626	$4p^3P_2 \rightarrow 4s^3D_2$	2294.364
	1626	$4p^3P_2 \rightarrow 4s^3D_3$	2246.995
Kr^+	(no levels in Cu II)		
Xe^+	(no levels in Cu II)		

Type 2 atom-atom collisions, that is, those involving metastable levels in the noble gas, have also been investigated by us. Again we have chosen to study copper and have used Shenstone's data to correlate collision processes with spectral emission. Instead of an alignment between Cu energy levels and noble gas ionization potentials, these collisions require aligning the Cu levels

with metastable levels in the gases. In helium the $^1S_0$ and $^3S_1$ states are metastable; and in neon, argon, krypton, and xenon the first four excited states are metastable at pressures above 0.01 mmHg due to resonance trapping.[9] The four levels are the $^1P_1[1s_2]$, $^3P_0[1s_3]$, $^3P_1[1s_4]$, and $^3P_2[1s_5]$, where the Paschen notation is given in brackets.

After seeking energy coincidences between the rare gas metastable levels mentioned above and the levels of Cu II and after looking for strong emission from the resonant copper levels, the following processes have been identified:

$$He(^3S_1) + Cu \rightarrow Cu^+(4s^2\ ^1G_4) + He + e^-$$

$$Ne(^1P_1) + Cu \rightarrow Cu^+(4p\ ^1P_1) + Ne + e^-$$

The energy discrepancy, ΔE, for the first collision is 1967.5 cm^{-1} and for the second 22.4 cm^{-1}. In each case the copper atom is ionized and left in an excited state. The copper ion in the $4s^2\ ^1G_4$ state radiates at three visible wavelengths; and from the $4p\ ^1P_1$ state, emission is at one wavelength in the ultraviolet:

$$\begin{aligned} 4s^2\ ^1G_4 &\rightarrow 4p\ ^3F_3 \text{ at } 3686.555\ \text{Å} \\ &\rightarrow 4p\ ^3D_3 \text{ at } 4043.502\ \text{Å} \\ &\rightarrow 4p\ ^1F_3 \text{ at } 4227.936\ \text{Å} \end{aligned}$$

$4p\ {}^1P_1 \rightarrow 4s\ {}^1D_2$ at 2112.090 Å

No energy resonances were found for argon, krypton, or xenon which would produce optical transitions in copper. Note that the energy level difference of 1967.5 cm^{-1} for the helium-copper resonance is too large to allow this process to occur in 400° atoms.

One fact which has not as yet been mentioned explicitly should be stated here. The gain coefficient of a laser medium can be shown to be proportional to the square of the operating wavelength, making it easiest to achieve laser action on long wavelength transitions. On this basis the 2112 Å line in Cu II would be discarded as a possible laser transition. Also the copper lines listed in Table 2 which are excited through the charge transfer process in Ne and A would be poor choices as laser transitions, situated as they are in the ultraviolet.

3.2 b Aluminum

Singly ionized aluminum has been found to collide with neon through a charge transfer process[10] which populates the 5^1P_1 state in Al II and gives rise to the transition $5^1P_1 \rightarrow 4^1D_2$ at a wavelength of 6335.70 Å. The 4^1D_2 state in turn decays to the 3^1P with emission at 1989.85 Å.[11] While other resonance collisions may be possible in aluminum, no investigations of energy levels were carried out by us since a low sputtering rate makes the metal a poor choice as a laser medium.

CHAPTER IV

EXPERIMENTAL RESULTS

4.1 Apparatus

In this chapter the bulk of our experimental data is presented. Some of the graphs were prepared specifically to test the straight line theory developed in Chapter 2, while others cover a variety of measurements which were made simply to gain a better understanding of the characteristics of the discharge tubes.

Figure 2 shows schematically the apparatus employed to record spectral line intensities. A copper hollow cathode tube is positioned at the entrance slit of the 750 mm Czerny-Turner spectrometer. The black portion of the discharge tube represents the hollow cathode. In all, a total of five tubes was used, four with copper and one with a kovar (iron, nickel, cobalt alloy) cathode. The voltage-current characteristic of one of the copper tubes is shown in Figure 3. Because gas atoms are easily trapped by the copper lattice as the discharge is run, the pressure falls quite rapidly in the copper cathode discharge tubes. A typical gas clean-up rate is plotted in Figure 4. To maintain operation, then, it is necessary to admit additional gas from time to time. To this end, a reservoir flask was added, from which gas could be

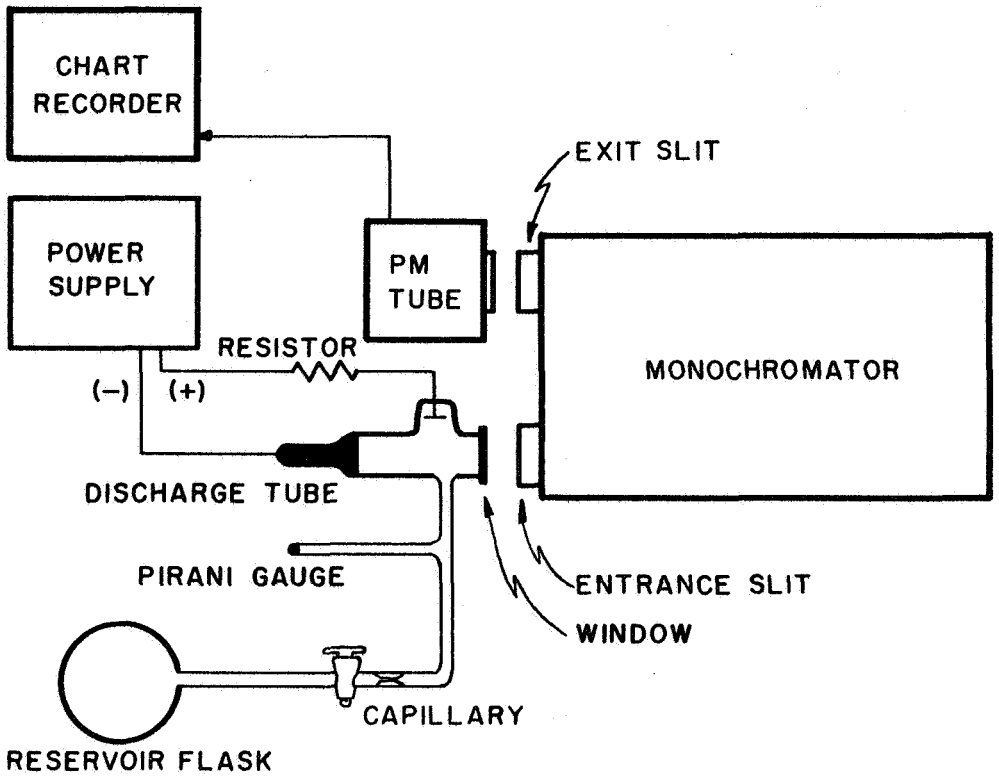

Figure 2. Apparatus Used for Spectral Measurements

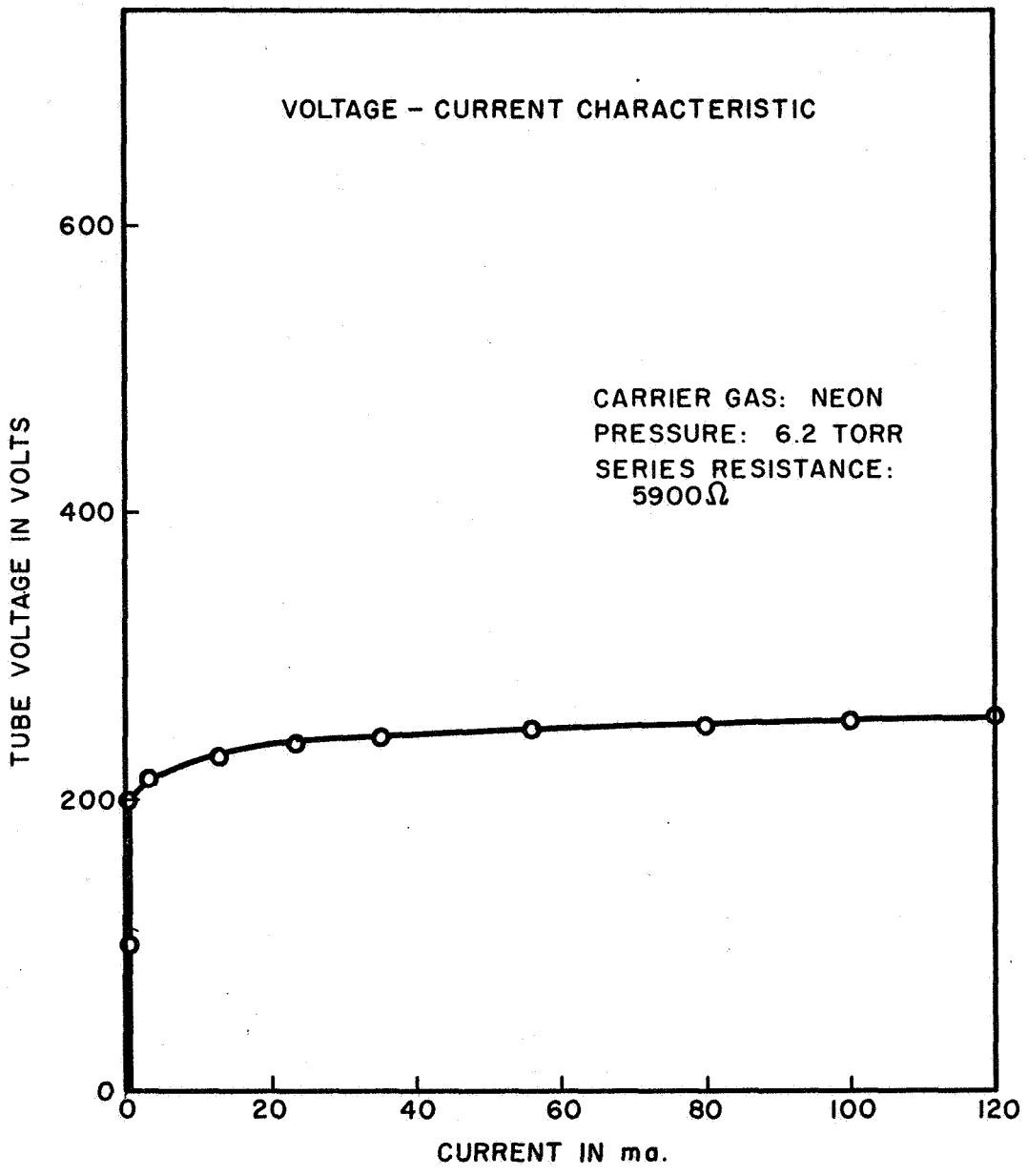

Figure 3. Voltage-Current Characteristic of Copper Cathode Discharge Tube

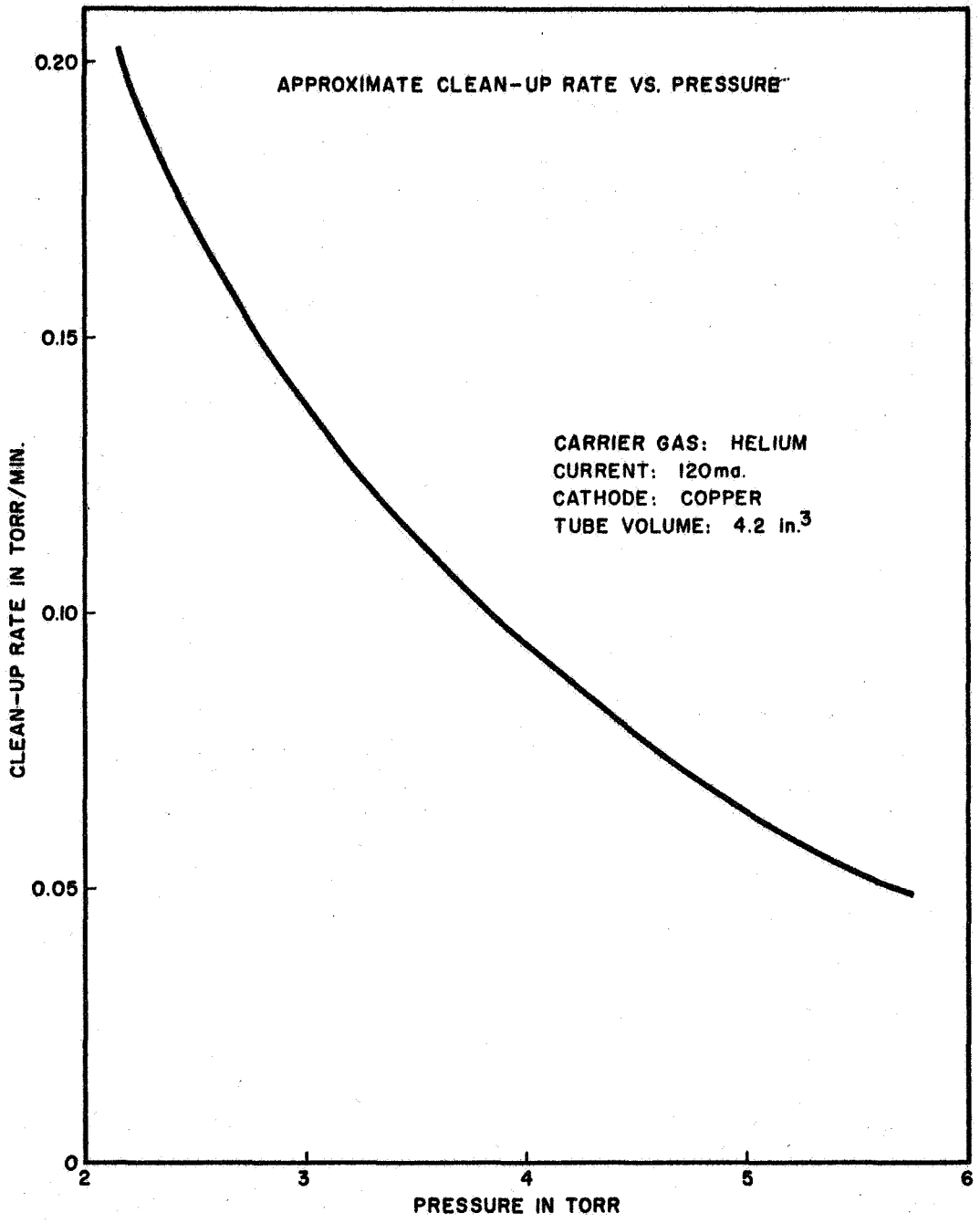

Figure 4. Carrier Gas Clean-up Rate

drawn through a stopcock and capillary. Gas pressure in the tube was continuously monitored with a Pirani gauge.

4.2 Graphs of Spectral Line Intensity Versus Excitation Energy

4.2 a Copper

In this section the results of our measurements of metal spectra are given for copper cathode tubes. The cathodes were tubular in shape, one inch long with a 3/8 inch ID. One end was rounded off and closed while the other was flared out and sealed directly to the glass portion of the discharge tubes.

Figures 5, 6, and 7 show the spectra of Cu I in argon, neon, and helium, respectively. Each data point on the graphs represents a single spectral line. Lines originating from the same upper atomic level lie vertically above one another on the graphs. The points on the argon and neon graphs are distributed along straight lines, indicating that excitation of the copper levels was principally by copper-electron collisions with the electrons having a Maxwell-Boltzmann distribution. According to the theory of Chapter 2, the electron temperature is obtained from the slope of the straight line through the points. The temperatures are, as noted on the graphs, 6200°K and 5300°K. Normally, one expects considerably higher electron temperatures, around 20,000°K, in glow discharges. The discrepancy is explained by realizing that the copper vapor, having a lower ionization potential than the rare

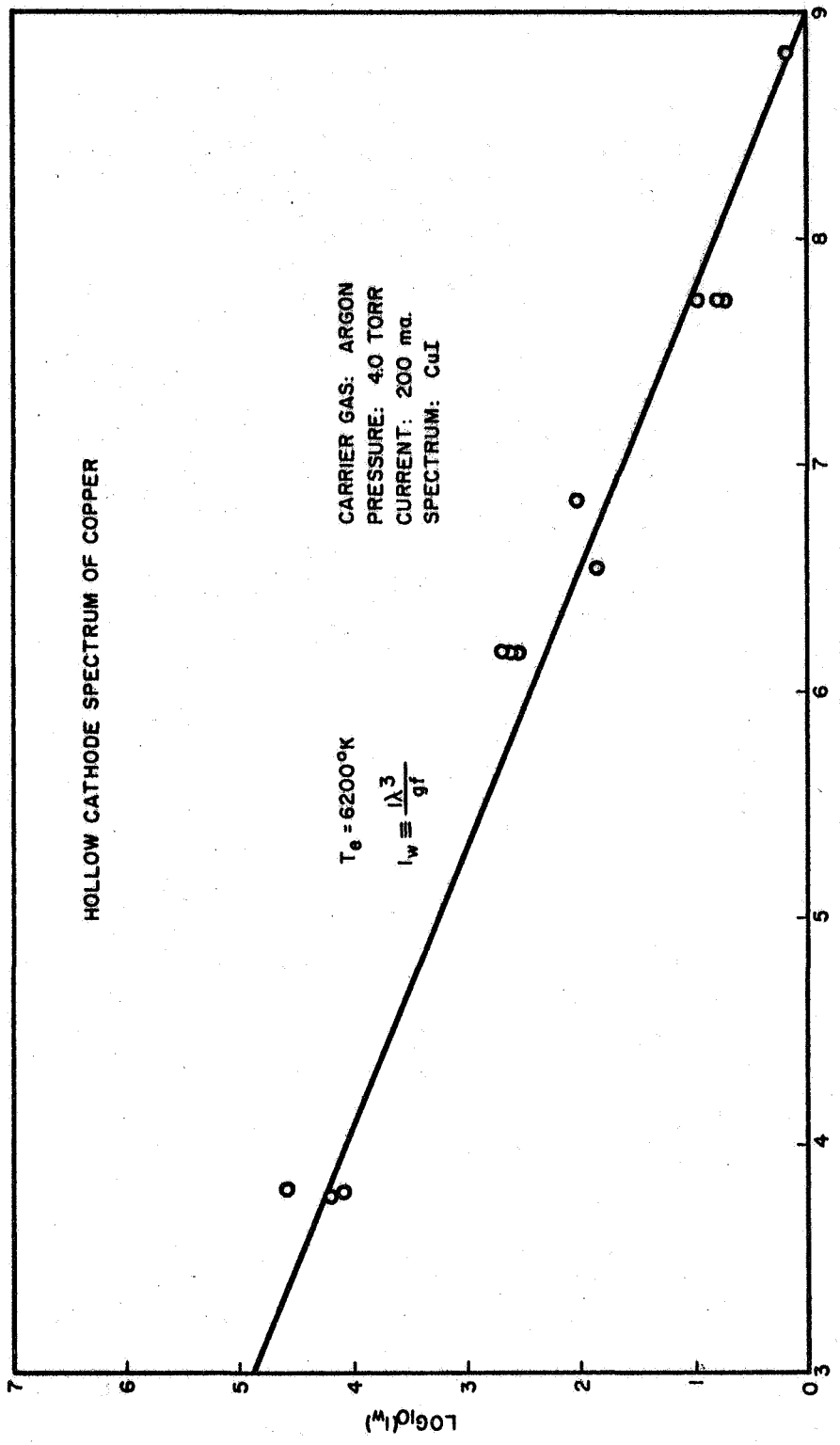

Figure 5. Copper Spectrum, Argon Discharge

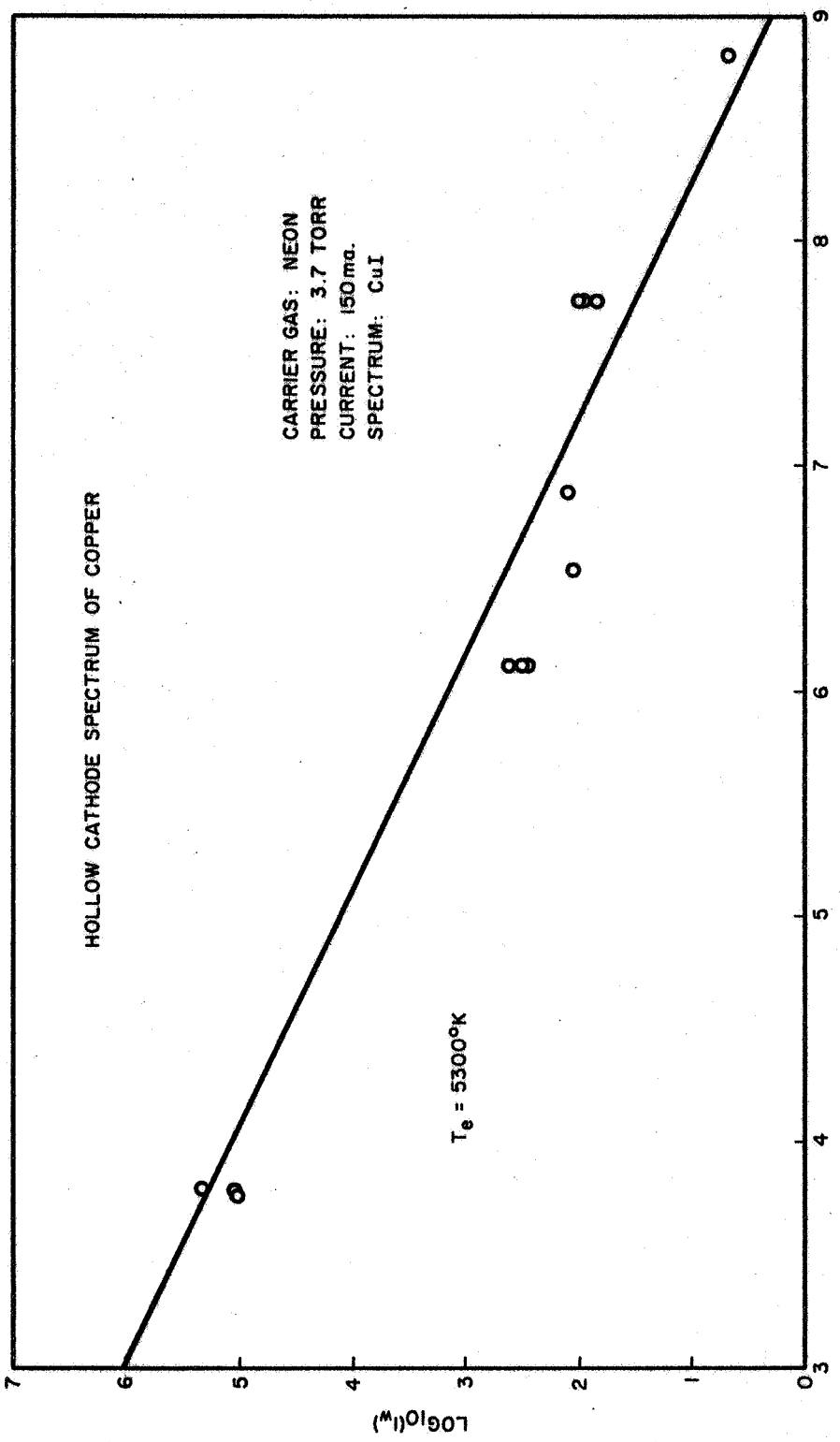

Figure 6. Copper Spectrum, Neon Discharge

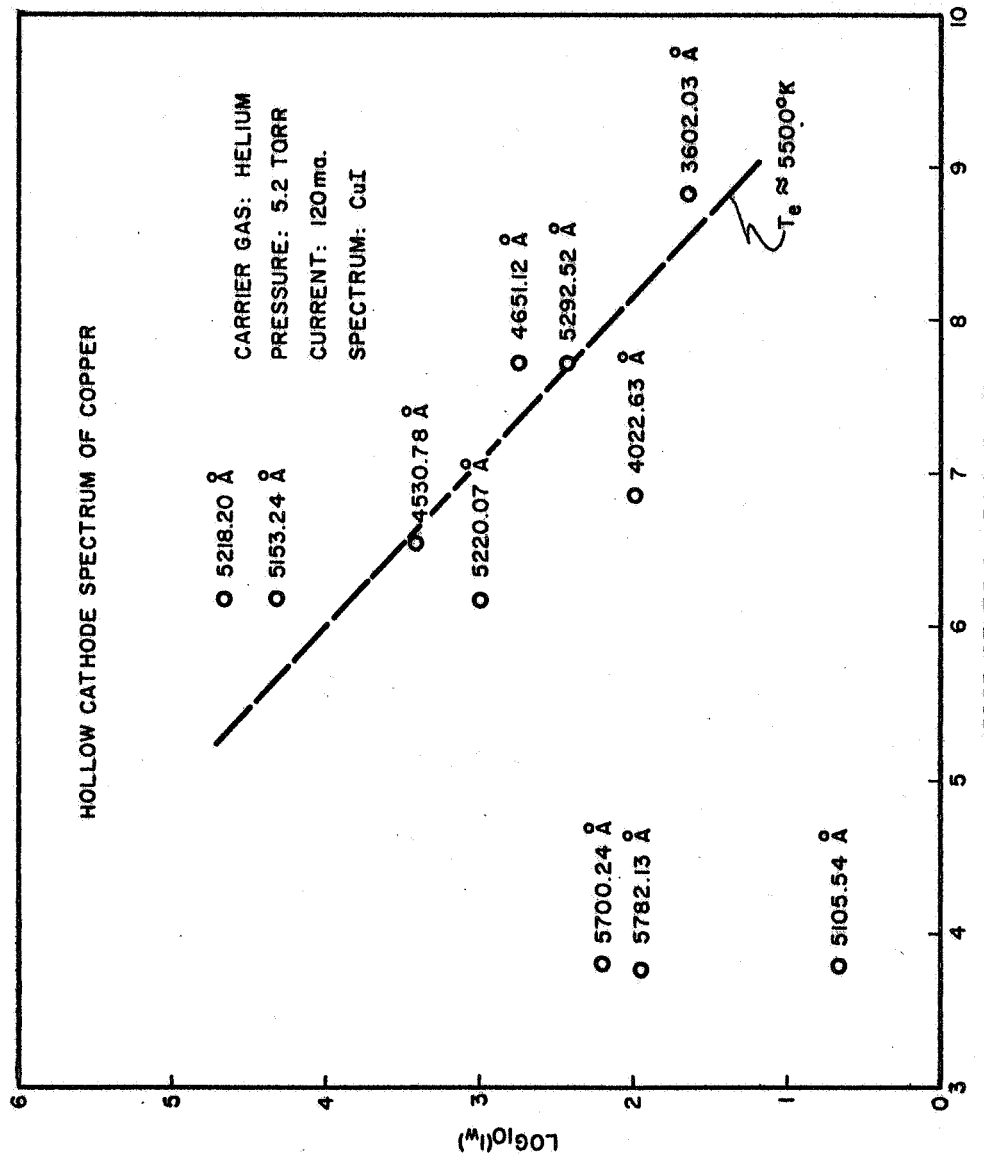

Figure 7. Copper Spectrum, Helium Discharge

gas has lowered the electron temperature near the cathode. In the positive column the temperature should be near the typical value.[12]

The generous scattering of the data points in the helium graph, without regard for a straight line, causes a slight dilemma. Where has the theory of Chapter 2 gone astray? Even those transitions from the same upper state do not appear with equal intensity.

The first culprit to suspect as a cause of the anomalous result is self-absorption. The transitions most likely to suffer self-absorption in the copper vapor would be those with a very low-lying lower level and those with a metastable lower level. The three points in Figure 7 in the lower left corner appear to be displaced by the greatest amount from their expected positions. Examination of the term scheme of copper reveals that the points represent transitions down to states near 1.5 ev, whereas all other points correspond to spectral lines having lower levels above 3.5 ev. In addition, the three levels are metastable since transitions to the ground state would violate the $\Delta L = 0, \pm 1$ selection rule. The lower level of the 5105 $\mathring{A}$ line is additionally metastable because a transition from this level to the ground state would violate $\Delta J = 0, \pm 1$, besides violating the rule for ΔL. Thus, self-absorption explains quite well the mislocation of these three points. What has caused the general spreading of the remaining points about the straight line is not clear.

4.2 b Iron

Eighteen iron lines observed with a kovar cathode discharge tube are plotted in Figure 8. All of the measured lines lay at the edge of the visible spectrum in the violet between 3443 Å and 4045 Å. The best straight line running through the graph points, in the sense of a minimum mean square error, gave an electron temperature of 3300°K. The one maverick point lying above the line was perhaps mistakenly identified as due to iron when, in reality, it may have been a weak helium line.

Figure 9 gives an estimate of the relative intensity of the iron spectrum as a function of pressure. The curve was measured with a prism spectrometer and photomultiplier which viewed a range of wavelengths in the violet where iron emission is strong while neon emission is very weak.

4.3 Spectral Line Intensities as Functions of Current

In order to gain further insight into the physical processes occurring within the hollow cathode tube it is instructive to observe the intensities of the spectral lines as functions of discharge current. We have, accordingly, measured the current dependence of several copper lines, the 5218 line of Cu I and the 4909 and 5941 lines of Cu II, and have looked briefly into the literature.[13] On the basis of these studies, some tentative ideas concerning the physics of the hollow cathode discharge are presented.

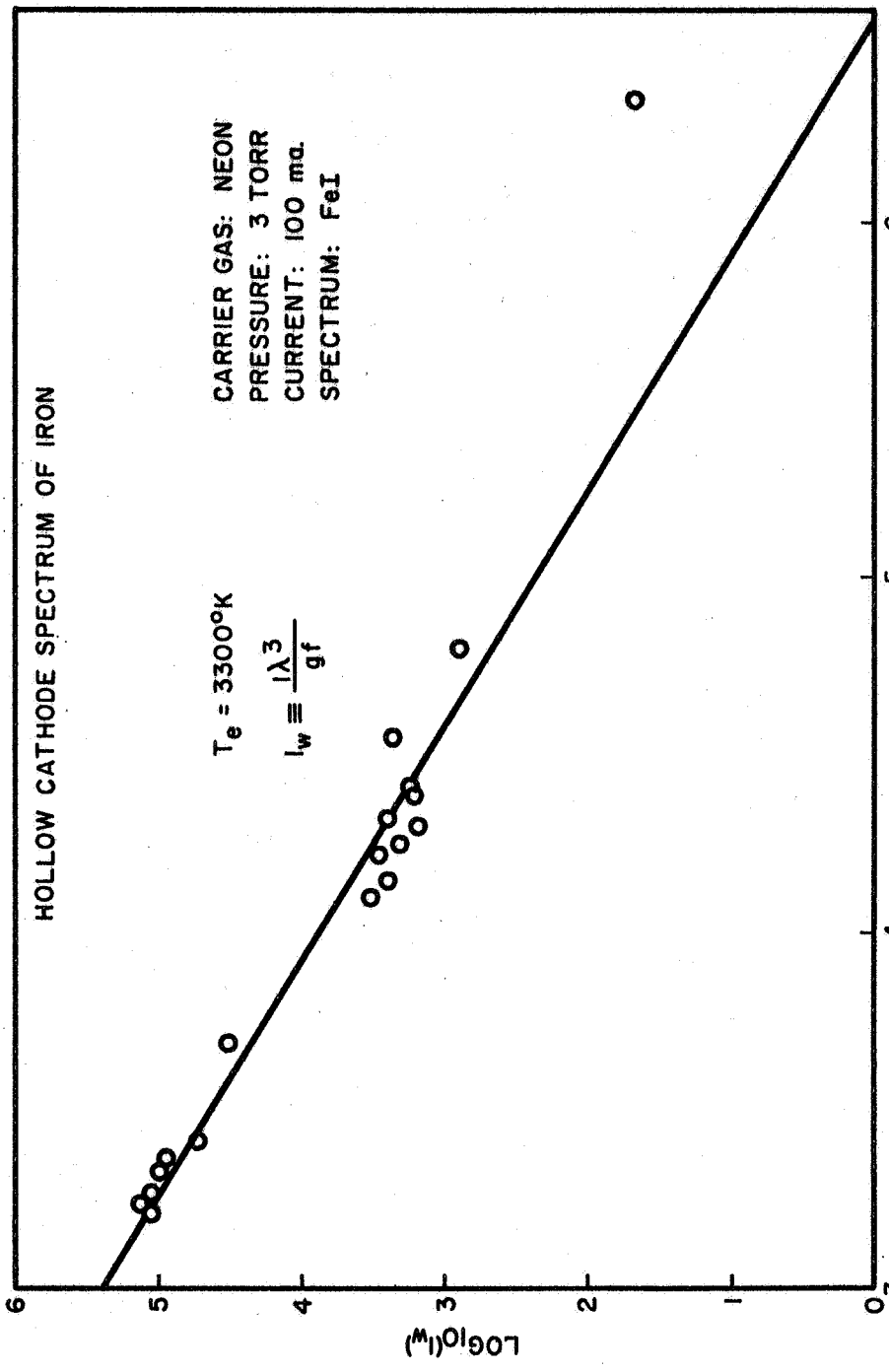

Figure 8. Iron Spectrum

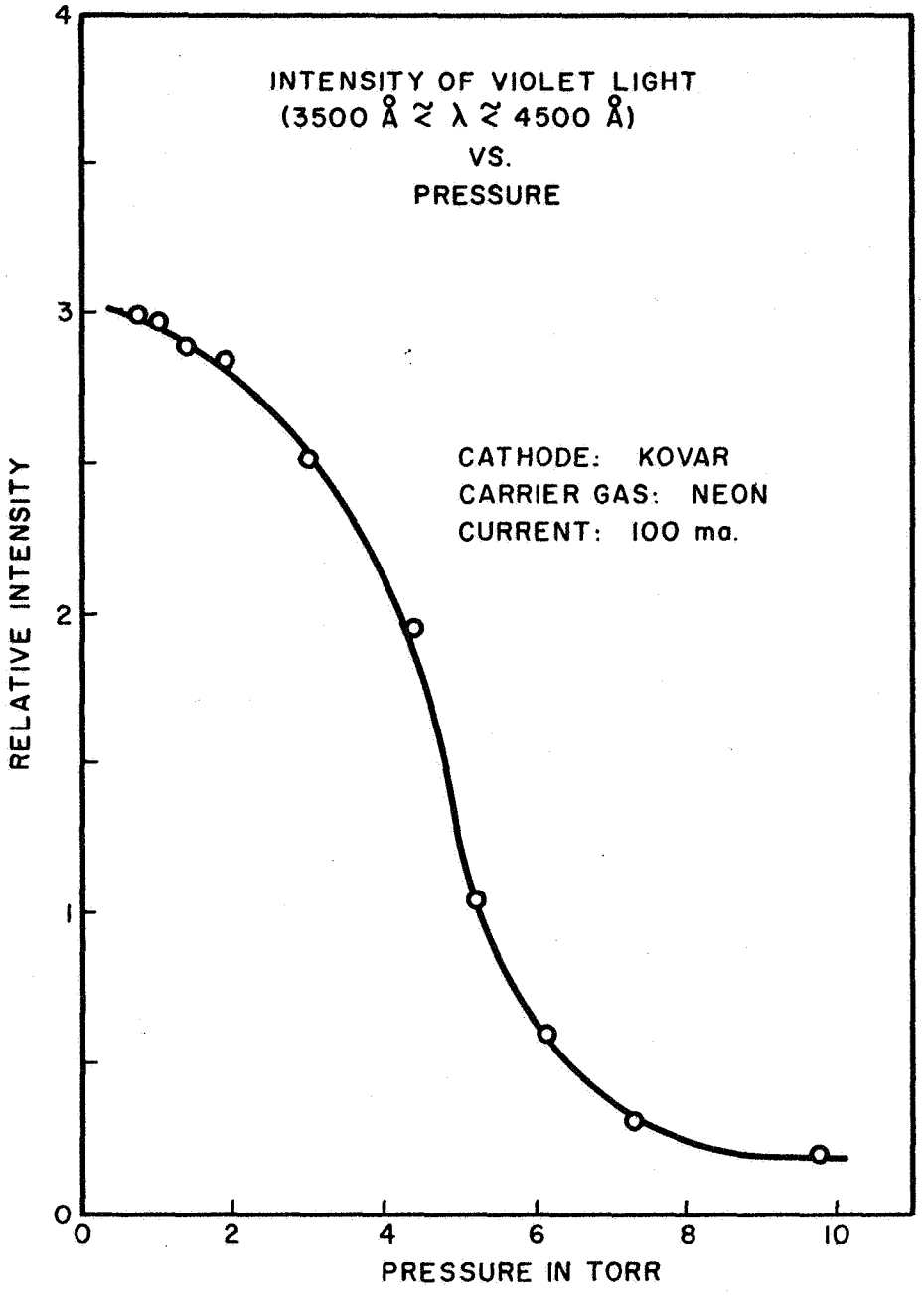

Figure 9. Intensity of Iron Emission

Electron densities within a hollow cathode structure may be on the order of 10^{12} electrons per cm^3 for currents of 100 ma. or more.[14] Furthermore, the electrons can be to some extent confined to the cathode region by space charge effects, giving rise to a nonlinear increase in cathode electron density with current. For a cathode consisting of two parallel molybdenum plates separated by 4 mm, T. Musha[15] has found the electron density to vary with the 1.7 power of the current. One explanation for the copious production of electrons is the occurrence of the photoelectric effect at the cathode wall. Ultraviolet radiation in the form of resonance lines from the metal and rare gas atoms does indeed possess sufficient energy for ejecting electrons. In fact, photoemission may amount to 75% or 80% of the total electron current.[16]

For the intensity of the spectral lines of the molybdenum cathode, Musha[17] has measured a cubic dependence on current, while for the carrier gas he found a nearly linear dependence. The fact that the intensity of the metal spectrum depended more strongly than the gas spectrum on the current suggests that the amount of molybdenum vapor increased toward higher currents due to stronger sputtering, whereas the amount of carrier gas was, of course, constant.

Figure 10 shows the variation in intensity of the 4909 Å copper ion line with discharge current and pressure. This is one of the transitions which would be excited, it was hoped, by charge transfer

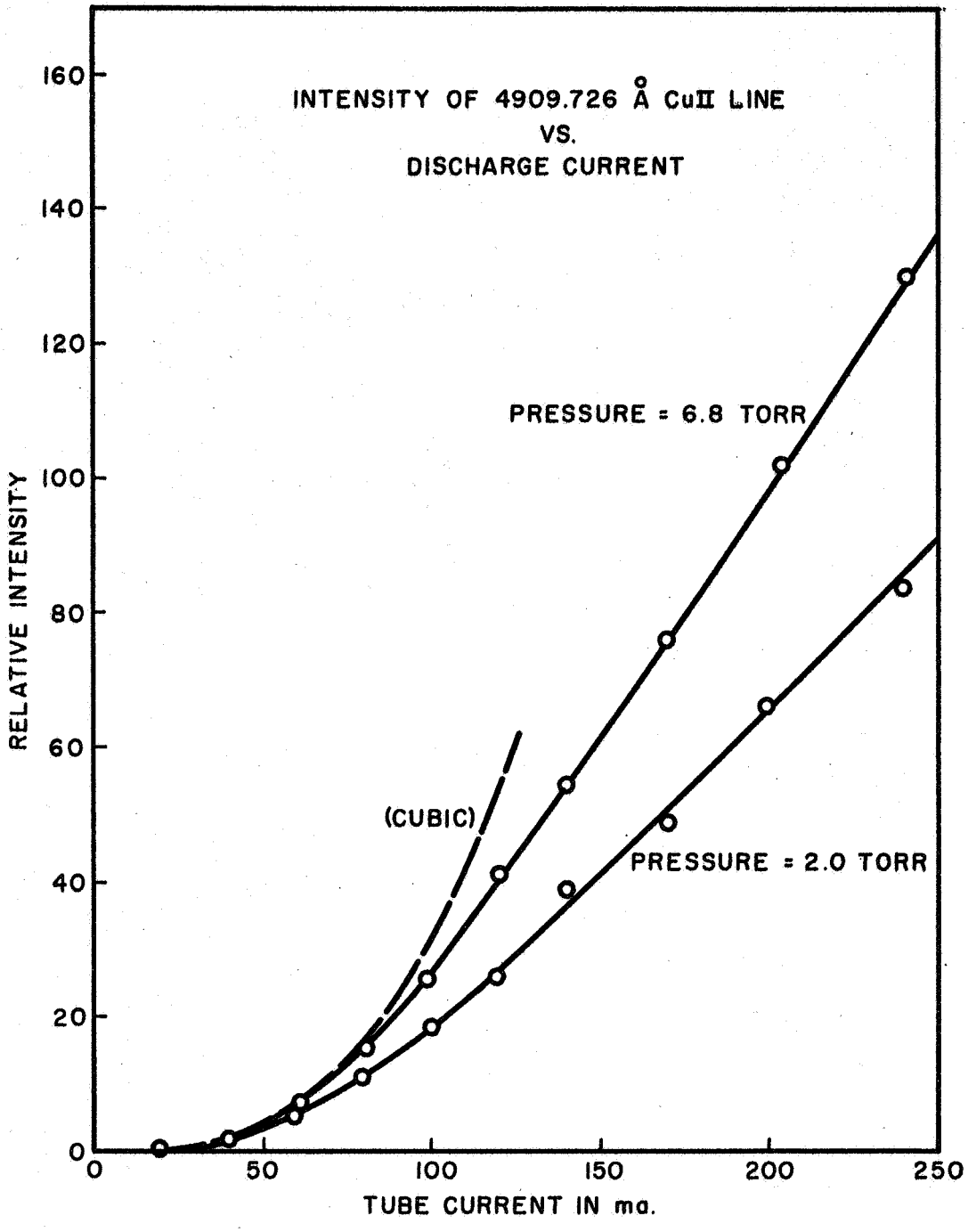

Figure 10. Intensity of 4909.726 Å Cu II Line

collisions with helium ions. Note that two distinct variations of intensity with current are evident, one below and one above 110 ma. The two regions are shown more clearly in Figure 11 which is a log-log plot of the 6.8 Torr curve of Figure 10. Also shown in Figure 11 is an intensity vs current curve for the 5941.17 Å line of Cu II. This line results from the decay of a level situated just above those which might be in resonance with He ions. The level should be populated by electron collisions rather than by the resonance process. The two curves are quite similar except that the slope of the 5941 curve changes at a higher value of current. The point at which the 5941 curve breaks toward a smaller slope is near 200 ma. at the upper end of the curve. On the basis of Figure 11, it is difficult to say whether or not the charge transfer process is exciting the 4909 line but not the 5941 line.

An interesting explanation involving the copper sputtering rate can be offered for the two regions of current dependence in Figure 11 -- the nearly cubic dependence at low currents and the smaller dependence at high currents. The explanation applies also to the Cu I line intensity curves of Figure 12. These curves show either quadratic or linear variations with current, depending on the carrier gas pressure.

As a starting point we write a simplified rate equation for the population density of the $4f\,^3H_6$ state of Cu II, which is the upper state for the 4909 transition. The number density of the

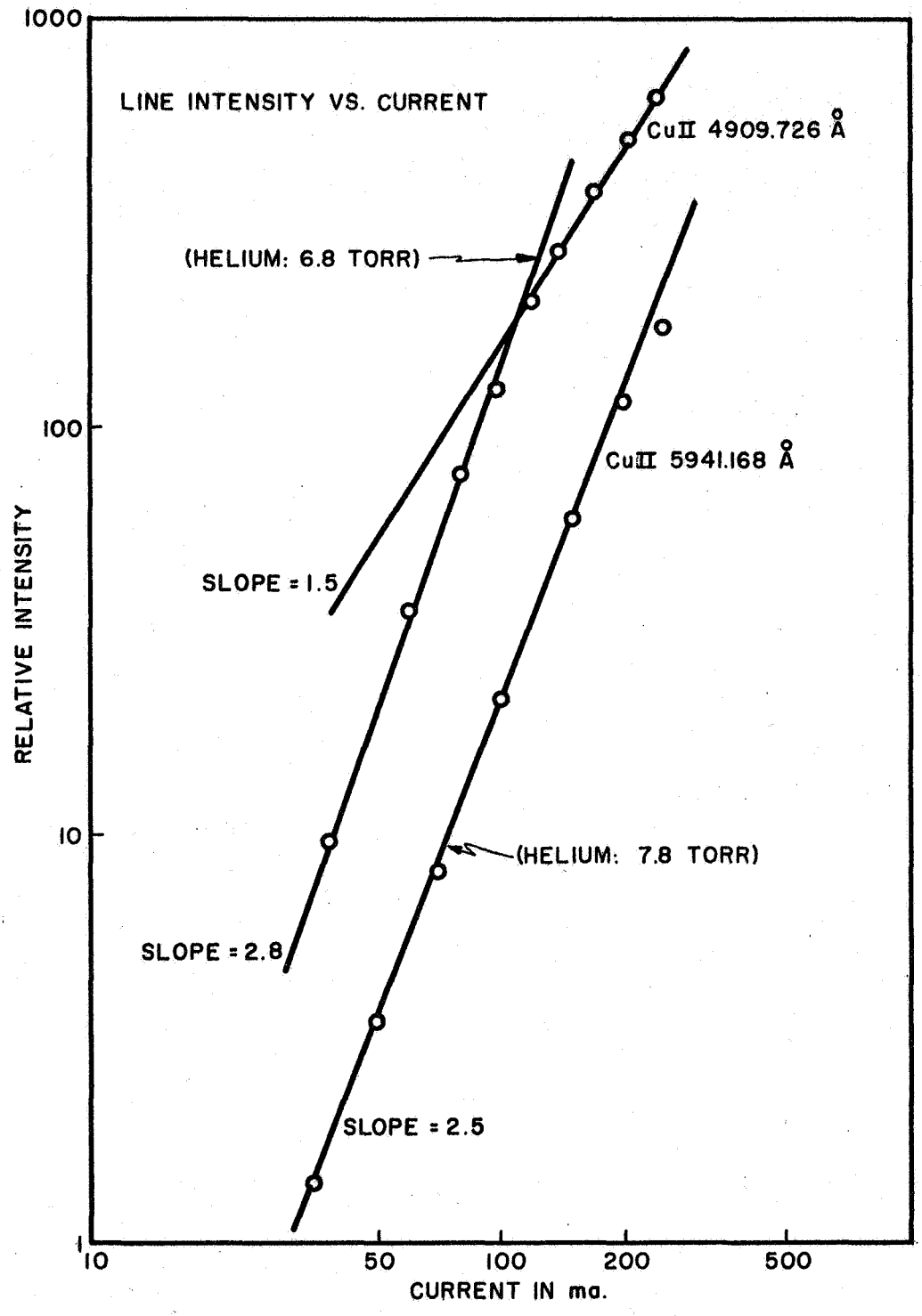

Figure 11. Intensities of 4909.726 Å and 5941.168 Å Cu II Lines

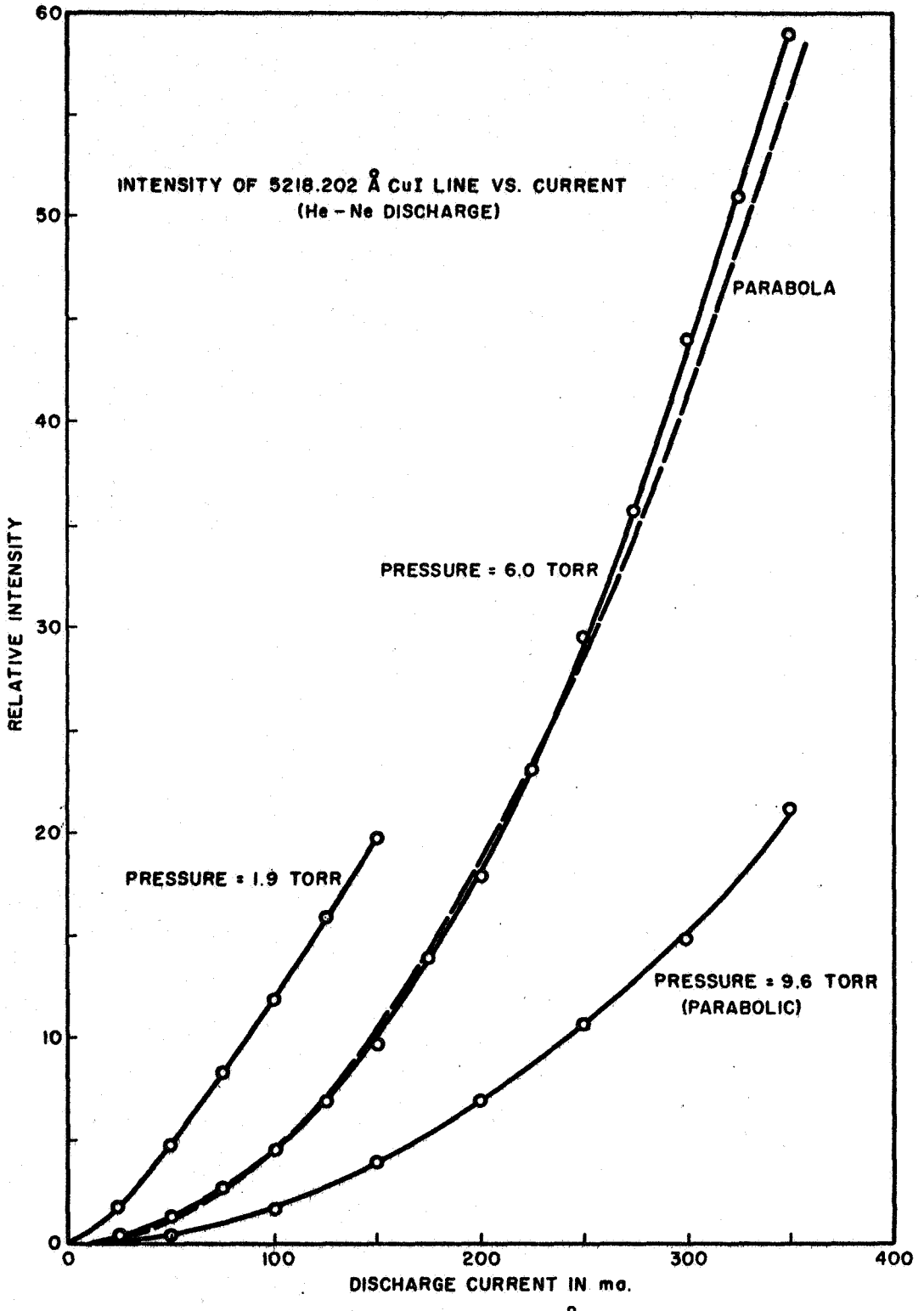

Figure 12. Intensity of 5218.202 Å Cu I Line

$4f^3H_6$ state is labeled n_2. Thus,

$$\frac{dn_2}{dt} = - A_{21}n_2 + n_e^2 n_o P_c \ , \qquad (4.1)$$

where A_{21} is the spontaneous transition probability for the 4909 line, n_e and n_o are the number densities of electrons and ground state copper atoms, respectively, and P_c is the collision probability for collisions that populate the $4f^3H_6$ state. In general, a rate equation of this type contains a number of collision and radiative terms which specify how rapidly the excited state is filled and emptied by various processes. One such collisional term is shown in Eq. 4.1 and represents excitation by two successive collisions. The first collision is between a ground state copper atom and an electron; it either excites the copper atom to a metastable level or ionizes it. The second collision sends the ion or metastable atom up to the $4f^3H_6$ state.

An equation identical to Eq. 4.1 can be written for the upper state of the 5941 line. For the upper level of the 5218 transition shown in Figure 12, Eq. 4.1 would contain n_e in place of n_e^2 since the transition is from an atomic copper level lying at a low enough energy to be excited by a single collision with an electron.

In the steady-state, n_3 is a constant, so the left side of Eq. 4.1 vanishes. Transposing the term $A_{21}n_2$ to the left side

yields the relationship

$$A_{21}n_2 \propto n_e^2 n_o \ . \tag{4.2}$$

As noted in Chapter 2, $A_{21}n_2$ is proportional to the line intensity, I. Also, let us assume, as is normally done for glow discharges, that n_e is proportional to the discharge current, I_T. Then from Eq. 4.2 it follows that

$$I \propto I_T^2 n_o \ . \tag{4.3}$$

For the 5218 line of Cu I, the electron density, n_e, appears linearly in the rate equation, and hence

$$I \propto I_T n_o \ . \tag{4.4}$$

The final hypotheses for explaining, at least to some extent, the shapes of the curves in Figures 10, 11, and 12 are now set forth. It is reasonable to assume that the sputtering of copper atoms at the cathode surface results from the impact of helium ions and from those copper ions previously sputtered as atoms and then ionized. Whenever a helium ion sputters a copper atom, the copper vapor density is increased; but when a copper ion sputters a copper

atom, the ion very likely adheres to the cathode, with the result of no net increase in copper vapor density. At low currents and high gas pressures (pressures above 4 Torr), sputtering is mainly caused by helium ions because the helium number density is high; and the density of copper atoms in the gas phase increases with current:

$$n_o \propto I \, . \tag{4.5}$$

For sufficiently high currents, even though the pressure is high, the amount of copper vapor may become so great that sputtering is taken over by copper ions. The vapor density then reaches a saturation value and

$$n_o \simeq \text{constant.} \tag{4.6}$$

For lower pressures, the copper ions quickly take over the sputtering process as the discharge current is increased. Thus for moderate and high currents the vapor density reaches some maximum value, and Eq. 4.6 again holds.

The shapes of the curves in Figures 11 and 12 may now be seen to follow from Eqs. 4.3 and 4.4 with appropriate substitutions from Eqs. 4.5 and 4.6. In figure 11 the nearly cubic dependence is explained using Eqs. 4.3 and 4.5 which give

$$I \propto I_T^3 ,$$

wherein the cubic dependence arises from the two step excitation of Eq. 4.3 and the proportionality between metal vapor density and discharge current of Eq. 4.5. The 1.5 power dependence in Figure 11 is approximately shown by the quadratic result obtained by combining Eqs. 4.3 and 4.6:

$$I \propto I_T^2 .$$

The discrepancy between the 1.5 and 2.0 power laws is reasonable within the framework of the assumptions which were made. The change in slope of the 4909 and 5941 intensity curves occurs because the vapor density no longer increases with current once the sputtering process is dominated by copper ions.

In Figure 12 the linear, low pressure curve results from Eqs. 4.4 and 4.6 which assume single step excitation of the upper excited state and a saturation value for the copper vapor density. The quadratic variations are justified from Eqs. 4.4 and 4.5 which imply sputtering mainly by helium ions.

CHAPTER V

THE COPPER LASER

As described in Chapter I, section 3, an attempt was made to achieve laser action in the sputtered metallic vapor of a hollow cathode tube. Copper was chosen for the cathode and a mixture of helium and neon, five parts helium to one part neon, for the carrier gas. The laser tube design is shown schematically in Figure 13. The cathode consists of a one inch diameter copper bar, one foot in length, bored to a 1/4 inch ID. A row of cooling fins was machined on the outer surface of the bar. A kovar-to-glass seal was silver soldered to the cathode at each end, and a nickel anode was fixed inside the glass bulb extending from each seal.

It was felt that the copper-helium charge transfer process described in Chapter 3 might sufficiently invert the $4f\,^3H_6$ and $4d\,^3G_5$ levels in Cu II so that oscillation, at least on a pulsed basis, would result. The five to one gas mixture was a convenient choice since it is the same as that used in the 6328 Å He-Ne laser. The neon is quite desirable in the copper system since, by virtue of the larger mass of the Ne atoms, a somewhat higher sputtering rate is expected.

Both pulse and continuous excitation techniques were tried.

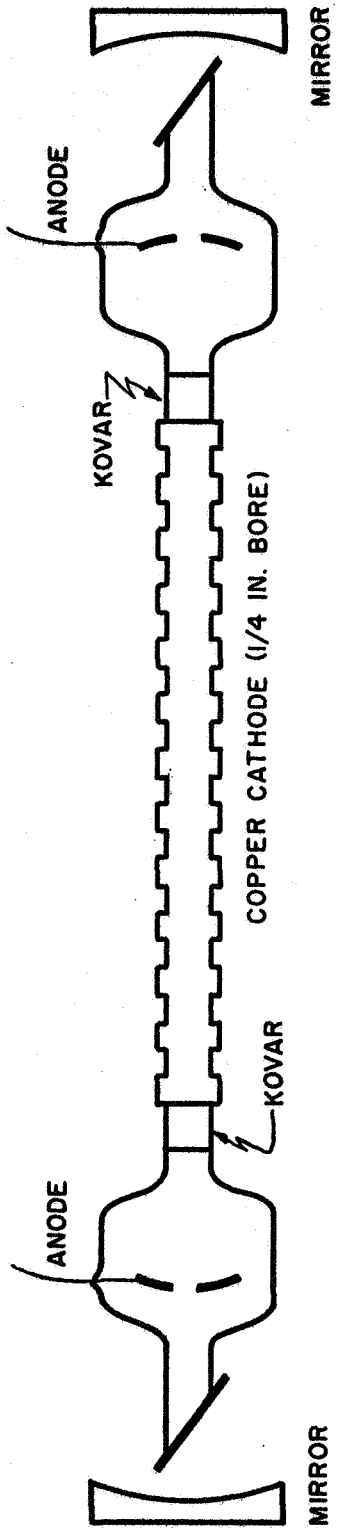

Figure 13. The Copper Laser

For pulsed operation the anodes were connected together and driven with 50 ampere, 1 microsecond pulses from a 750 kilowatt magnetron supply. No series resistance was needed. A maximum pulse repetition rate of 1000 pps was used, and discharge pressures were varied between one and ten Torr. For DC excitation, each anode was placed in series with a 2000 ohm resistor bank and total currents of up to 1.6 amp. were run. At gas pressures above 1 Torr, the discharge was concentrated within the bore of the cathode, with only a faint glow visible on the surface of the anode. That is, there was essentially no positive column but only a bright negative glow. For currents in excess of 1.3 amp. and with the discharge pressure at or near 3.5 Torr, the negative glow changed from bright red-orange to an intense green, indicating strong enhancement of the copper spectrum. The three strong green lines of Cu I were, in fact, the brightest lines which could be observed with a pocket spectroscope. It is quite possible that as the current reached the 1.3 amp. value, the sputtering process was taken over by copper ions which eject copper atoms very efficiently from the cathode surface, with the result of a greatly increased copper vapor density and increased copper emission.

Two comments are now in order regarding the failure of the above procedures in attaining laser action. First, it was discovered that trace amounts of copper had been deposited on the laser windows as a result of the normal operation of the discharge. Even

minute concentrations of foreign matter on the surfaces of windows can at times destroy laser action. Since no provision for preventing copper vapor from reaching the windows was made in our first laser design, the tube must be at least partially rebuilt. An obvious future step would be to lengthen the glass portions of the tube, thereby increasing the distance between cathode and windows.

As a second comment, we note that alignment of the mirrors is quite difficult on a large bore tube of the type used for the copper laser. It cannot be said with assurance that the mirrors were faithfully aligned throughout the various attempts at achieving a lasing discharge.

CHAPTER VI

CONCLUSIONS

In Chapter I section 2 a spectroscopic method was outlined which involved graphs of spectral line intensity versus upper state excitation energy. This approach could not be conveniently applied to the spectrum of singly ionized copper since gf-values are not available for the visible Cu II transitions. Thus, the extent to which the $4f\,^3H_6$ level in Cu II is populated through charge transfer with helium ions (as in process 1,Chapter 3 section 1) cannot be determined by this method. The graphical technique may find application in another area, namely the problem of determining unknown gf-values. How this may be accomplished can be understood as follows: Assume that gf-values are known for a few transitions in a particular atomic species. If the intensities of a number of spectral lines are measured, then, using those lines for which the gf-values are known, a graph of intensity versus upper state energy can be constructed. The electron temperature can be found from the slope of the best-fitting straight line. The graph points for all those spectral lines with unknown gf-values can then be placed on the straight line at the locations corresponding to their upper excitation energies, and the gf-values for the lines can be

determined. Such a scheme might be applied, for example, to Cu II, for which a small number of absolute gf-values are presently known for transitions in the ultraviolet. It would be necessary, however, before attempting such an experiment, to check for energy coincidences between the levels of Cu II involved in the ultraviolet transitions and the metastable levels in the carrier gas. If resonance collisions were associated with these levels, an incorrect value of electron temperature, and thus incorrect gf-values, might result. Notice that in this technique one utilizes a certain number of gf-values which are already known in an absolute sense and thus is able to compute absolute rather than relative numbers for the unknown gf-values.

From Figures 5, 6, and 8 it seems clear that the electrons within the copper-argon, copper-neon, and iron-neon discharges were indeed in a near equilibrium regime. For the copper cathodes, it was the argon discharge which provided the lesser amount of scattering of the data points about the straight line. On this basis, one would probably want to try argon as the carrier gas for the experimental determination of Cu II gf-values mentioned in the preceding paragraph.

From the standpoint of a copper laser, the helium discharge of Figure 7 appears to be most promising. The strong self-absorption of the 5700, 5782, and 5105 lines represents a significant density of ground state and near ground state copper atoms in the gas phase.

This indicates that the total copper vapor density is greatest, and in fact quite high, in the helium discharge.

As discussed in Chapter 3, the work of Shenstone reveals the presence of various resonant collision phenomena and in particular reveals a charge transfer collision between helium ions and copper atoms which populates the $4f^3H_6$ and $4f^3H_5$ levels in Cu II and causes intense copper emission at 4909 Å and 4931 Å. These lines are of primary interest as possible laser wavelengths. Other resonance collisions between copper and helium and between copper and neon are apparent in Shenstone's data, but most excite only very weak transitions or transitions situated too far in the ultraviolet for laser use.

Research on the copper laser is to be continued. In particular, after modifying the laser tube by increasing the length of the glass sections as described in Chapter 5, DC discharges are to be run with the simultaneous injection of high-current pulses. The high DC level should maintain a dense cloud of copper vapor within the bore of the cathode while the current pulses provide energetic electrons for exciting the copper levels. It is possible that pulsed laser oscillation will be achieved by this scheme on atomic copper transitions rather than on ionic transitions excited through the copper-helium charge transfer process. Recently pulsed laser action has been reported[18] at the 5105 and 5782 lines of Cu I. The copper was excited directly by collisions with high energy electrons,

which pumped the copper levels essentially according to optical selection rules.

FOOTNOTES

1. F. Paschen, "Die Funkenspektren des Aluminium," Annalen der Physik, 71 (November, 1923), p. 143.

2. David J. Rose and Melville Clark Jr., Plasmas and Controlled Fusion (New York: John Wiley and Sons, Inc., 1961),p. 49.

3. Toshimitsu Musha, "Cathode Sputtering in Hollow Cathode Discharges," Journal of the Physical Society of Japan, 17 (September, 1962), p. 1444.

4. S. Tolansky, High Resolution Spectroscopy (London: Methuen and Co., Ltd., 1947), p. 115.

5. A. G. Shenstone, "The First Spark Spectrum of Copper," Philosophical Transactions of the Royal Society of London, 235, Series A (1936), pp. 195-243.

6. Lawrence H. Aller, Astrophysics: The Atmospheres of the Sun and Stars (New York: Ronald Press Co., 1963), Chapter 4.

7. Charles A. Corliss and William R. Bozman, Experimental Transition Probabilities for Spectral Lines of Seventy Elements, National Bureau of Standards Monograph 53 (Washington: U.S. Government Printing Office, 1962), p. 80.

8. Shenstone, pp. 195-243.

9. W. R. Bennett Jr., "Gaseous Optical Masers," Applied Optics, Supplement 1: Optical Masers (1962), p. 51.

10. Allan C. Mitchell and Mark W. Zemansky, Resonance Radiation and Excited Atoms (Cambridge Eng.: University Press, 1934), p. 220.

11. R. A. Sawyer and F. Paschen, "Das erste Funkenspektrum des Aluminiums Al II," Annalen der Physik, 84 (September, 1927), p. 16.

12. Pointed out by Dr. Carl Kenty of General Electric in a personal conversation.

13. Musha, pp. 1440-1446.

14. Ibid., p. 1445.

15. Ibid., p. 1445.

16. V. K. Rohatgi, "Electronic and Ionic Current at the Cathode of a Hollow-Cathode Discharge," Journal of Applied Physics, 32 (June, 1961), p. 1173.

17. Musha, p. 1441.

18. W. T. Walter, et.al., Efficient Pulsed Gas Discharge Lasers, A Report to the International Quantum Electronics Conference, Phoenix, Arizona, April 12 to April 15, 1966, Prepared by Control Data Corporation (Melville, New York: The Conference, 1966), p. 43.

BIBLIOGRAPHY

Aller, Lawrence H., Astrophysics: The Atmospheres of the Sun and Stars. New York: Ronald Press Co., 1963.

Bennett, W. R. Jr., "Gaseous Optical Masers", Applied Optics, Supplement 1: Optical Masers, (1962), 24-62.

Corliss, Charles H. and William R. Bozman, Experimental Transition Probabilities for Spectral Lines of Seventy Elements. National Bureau of Standards Monograph 53. Washington: U.S. Government Printing Office, 1962.

Mitchell, Allan C., and Mark W. Zemansky, Resonance Radiation and Excited Atoms. Cambridge, Eng.: University Press, 1934.

Musha, Toshimitsu, "Cathode Sputtering in Hollow Cathode Discharges," Journal of the Physical Society of Japan, 17 (September, 1962), 1440-1446.

Paschen, F. "Die Funkenspektren des Aluminium". Annalen der Physik, 71 (November, 1923), 142-161.

Rohatgi, V. K., "Electronic and Ionic Current at the Cathode of a Hollow-Cathode Discharge". Journal of Applied Physics, 32 (June, 1961), 1173-1174.

Rose, David J. and Melville Clark Jr., Plasmas and Controlled Fusion. New York: John Wiley and Sons, Inc. 1961.

Sawyer, R. A. and F. Paschen, "Das erste Funkenspektrum des Aluminiums Al II." Annalen der Physik, 84 (September, 1927, 1-19.

Shenstone, A. G., "The First Spark Spectrum of Copper". Philosophical Transactions of the Royal Society of London, 235, series A (1936), 195-243.

Tolansky, S., High Resolution Spectroscopy. London: Methuen and Co., Ltd., 1947.

Walter, W. T.,N. Solimene, M. Piltch and G. Gould, Efficient Pulsed Gas Discharge Lasers. A Report to the International Quantum Electronics Conference, Phoenix, Arizona, April 12 to April 15, 1966. Prepared by Control Data Corporation. Melville, New York, 1966.